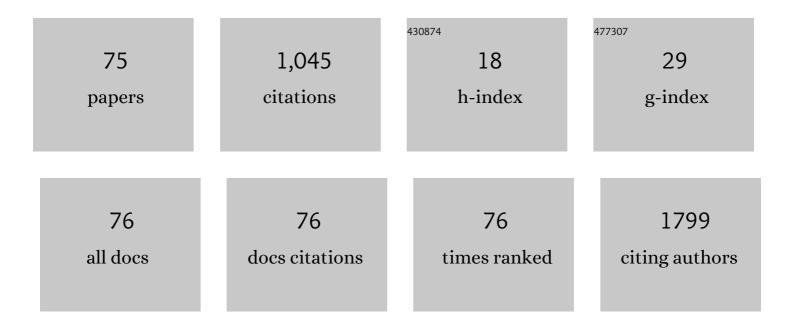
Huadan Xue

List of Publications by Year in descending order

Source: https://exaly.com/author-pdf/1588745/publications.pdf Version: 2024-02-01



Ημαράνι Χμε

#	Article	IF	CITATIONS
1	Histogram Analysis Based on Apparent Diffusion Coefficient Maps of Bone Marrow in Multiple Myeloma: An Independent Predictor for High-risk Patients Classified by the Revised International Staging System. Academic Radiology, 2022, 29, e98-e107.	2.5	2
2	Prediction of Early Treatment Response in Multiple Myeloma Using MY-RADS Total Burden Score, ADC, and Fat Fraction From Whole-Body MRI: Impact of Anemia on Predictive Performance. American Journal of Roentgenology, 2022, 218, 310-319.	2.2	14
3	M <mml:math <br="" xmlns:mml="http://www.w3.org/1998/Math/MathML">altimg="si1.svg"><mml:msup><mml:mrow></mml:mrow><mml:mn>3</mml:mn></mml:msup></mml:math> Net: A multi-scale multi-view framework for multi-phase pancreas segmentation based on cross-phase non-local attention. Medical Image Analysis. 2022. 75. 102232.	11.6	17
4	CT-based radiomics model for preoperative prediction of hepatic encephalopathy after transjugular intrahepatic portosystemic shunt. British Journal of Radiology, 2022, 95, 20210792.	2.2	4
5	Clinical effectiveness of contrast medium injection protocols for 80-kV coronary and craniocervical CT angiography—a prospective multicenter observational study. European Radiology, 2022, 32, 3808-3818.	4.5	5
6	Diffuse Involvement of Pancreas is not Always Autoimmune Pancreatitis. Academic Radiology, 2022, 29, 1523-1531.	2.5	4
7	A deep learning algorithm to improve readers' interpretation and speed of pancreatic cystic lesions on dual-phase enhanced CT. Abdominal Radiology, 2022, , 1.	2.1	6
8	Assessment of facial autologous fat grafts using Dixon magnetic resonance imaging. Quantitative Imaging in Medicine and Surgery, 2022, 12, 2830-2840.	2.0	1
9	Optical magnetic multimodality imaging of plectin-1-targeted imaging agent for the precise detection of orthotopic pancreatic ductal adenocarcinoma in mice. EBioMedicine, 2022, 80, 104040.	6.1	14
10	Serial Circulating Tumor DNA in Predicting and Monitoring the Effect of Neoadjuvant Chemoradiotherapy in Patients with Rectal Cancer: A Prospective Multicenter Study. Clinical Cancer Research, 2021, 27, 301-310.	7.0	65
11	Distinguishing pancreatic cancer and autoimmune pancreatitis with in vivo tomoelastography. European Radiology, 2021, 31, 3366-3374.	4.5	27
12	Baseline bone marrow ADC value of diffusion-weighted MRI: a potential independent predictor for progression and death in patients with newly diagnosed multiple myeloma. European Radiology, 2021, 31, 1843-1852.	4.5	19
13	Quick evaluation of lower leg ischemia in patients with peripheral arterial disease by time maximum intensity projection CT angiography: a pilot study. BMC Medical Imaging, 2021, 21, 7.	2.7	1
14	Blood supply of the male breast nipple-areola complex evaluated by CTA. Journal of Plastic, Reconstructive and Aesthetic Surgery, 2021, 74, 2588-2595.	1.0	2
15	Tumor Volume Predicts High-Risk Patients and Guides Initial Chemoradiotherapy for Early Cervical Cancer. Frontiers in Oncology, 2021, 11, 640846.	2.8	2
16	DWI of Autoimmune Pancreatitis: Is It an Imaging Biomarker for Disease Activity?. American Journal of Roentgenology, 2021, 216, 1240-1246.	2.2	3
17	Endometrial T2 values and thickness measured during the spontaneous menstrual cycle: potential imaging biomarker related to female physiological hormones. Chinese Journal of Academic Radiology, 2021, 4, 98-104.	0.6	1
18	Feasibility evaluation of amide proton transfer-weighted imaging in the parotid glands: a strategy to recognize artifacts and measure APT value. Quantitative Imaging in Medicine and Surgery, 2021, 11, 2279-2291.	2.0	5

#	Article	IF	CITATIONS
19	Comparison of image quality and lesion diagnosis in abdominopelvic unenhanced CT between reduced-dose CT using deep learning post-processing and standard-dose CT using iterative reconstruction: A prospective study. European Journal of Radiology, 2021, 139, 109735.	2.6	10
20	Parallel Medical Imaging: An ACP-Based Approach for Intelligent Medical Image Recognition with Small Samples. , 2021, , .		2
21	Imaging Features of Breast Periductal Stromal Tumor: A Case Report. Frontiers in Oncology, 2021, 11, 577227.	2.8	2
22	Application of Compressed Sensing 3D MR cholangiopancreatography (CS-MRCP) with Contact-Free Physiological Monitoring (CFPM) for Pancreaticobiliary Disorders. Academic Radiology, 2021, 28 Suppl 1, S148-S156.	2.5	1
23	Assessment of Response to Chemotherapy in Pancreatic Cancer with Liver Metastasis: CT Texture as a Predictive Biomarker. Diagnostics, 2021, 11, 2252.	2.6	1
24	The association of different serum IgG4 levels with distinct clinical characteristics and treatment efficacy in patients with IgG4-related disease. Clinical and Experimental Rheumatology, 2021, 39, 727-735.	0.8	0
25	Development of a Prognostic Nomogram in Hepatocellular Carcinoma with Portal Vein Tumor Thrombus Following Trans-Arterial Chemoembolization with Drug-Eluting Beads. Cancer Management and Research, 2021, Volume 13, 9367-9377.	1.9	2
26	Using amide proton transfer-weighted MRI to non-invasively differentiate mismatch repair deficient and proficient tumors in endometrioid endometrial adenocarcinoma. Insights Into Imaging, 2021, 12, 182.	3.4	3
27	Comparison and evaluation of the efficacy of compressed SENSE (CS) and gradient―and spinâ€echo (GRASE) in breathâ€hold (BH) magnetic resonance cholangiopancreatography (MRCP). Journal of Magnetic Resonance Imaging, 2020, 51, 824-832.	3.4	25
28	Initial Clinical Experience of Virtual Monoenergetic Imaging Improves Stent Visualization in Lower Extremity Run-Off CT Angiography by Dual-Layer Spectral Detector CT. Academic Radiology, 2020, 27, 825-832.	2.5	5
29	Multiparametric MRIâ€Based Radiomics for Prostate Cancer Screening With PSA in 4–10 ng/mL to Reduce Unnecessary Biopsies. Journal of Magnetic Resonance Imaging, 2020, 51, 1890-1899.	3.4	50
30	CT texture analysis predicts abdominal aortic aneurysm post-endovascular aortic aneurysm repair progression. Scientific Reports, 2020, 10, 12268.	3.3	12
31	Morphological description of uterine scar 1Âyear after cesarean section by 3D-SPACE 3.0T MR. Chinese Journal of Academic Radiology, 2020, 3, 162-168.	0.6	1
32	Progress and prospect on imaging diagnosis of COVID-19. Chinese Journal of Academic Radiology, 2020, 3, 4-13.	0.6	46
33	Optimization of Simultaneous Multislice, Readout-Segmented Echo Planar Imaging for Accelerated Diffusion-Weighted Imaging of the Head and Neck: A Preliminary Study. Academic Radiology, 2020, 27, e245-e253.	2.5	5
34	Prospective Comparison of Reduced Field-of-View (rFOV) and Full FOV (fFOV) Diffusion-Weighted Imaging (DWI) in the Assessment of Insulinoma: Image Quality and Lesion Detection. Academic Radiology, 2020, 27, 1572-1579.	2.5	10
35	Identifying clinical subgroups in IgG4-related disease patients using cluster analysis and IgG4-RD composite score. Arthritis Research and Therapy, 2020, 22, 7.	3.5	13
36	Combination Immunotherapy with Cytotoxic T-Lymphocyte–Associated Antigen-4 and Programmed Death Protein-1 Inhibitors Prevents Postoperative Breast Tumor Recurrence and Metastasis. Molecular Cancer Therapeutics, 2020, 19, 802-811.	4.1	18

#	Article	IF	CITATIONS
37	Application of integrated positron emission tomography/magnetic resonance imaging in evaluating the prognostic factors of head and neck squamous cell carcinoma with positron emission tomography, diffusion-weighted imaging, dynamic contrast enhancement and combined model. Dentomaxillofacial Radiology, 2020, 49, 20190488.	2.7	3
38	Human and mouse studies establish TBX6 in Mendelian CAKUT and as a potential driver of kidney defects associated with the 16p11.2 microdeletion syndrome. Kidney International, 2020, 98, 1020-1030.	5.2	17
39	Laparoscopic resection of large retrorectal developmental cysts in adults: Single-centre experiences of 20 cases. Journal of Minimal Access Surgery, 2020, 16, 152.	0.7	5
40	Weight-adapted ultra-low-dose pancreatic perfusion CT: radiation dose, image quality, and perfusion parameters. Abdominal Radiology, 2019, 44, 2196-2204.	2.1	4
41	Differences and similarities between IgG4-related disease with and without dacryoadenitis and sialoadenitis: clinical manifestations and treatment efficacy. Arthritis Research and Therapy, 2019, 21, 44.	3.5	18
42	Comparison of biparametric and multiparametric MRI in the diagnosis of prostate cancer. Cancer Imaging, 2019, 19, 90.	2.8	50
43	Sex disparities in clinical characteristics and prognosis of immunoglobulin G4–related disease: a prospective study of 403 patients. Rheumatology, 2019, 58, 820-830.	1.9	57
44	TBX6 compound inheritance leads to congenital vertebral malformations in humans and mice. Human Molecular Genetics, 2019, 28, 539-547.	2.9	46
45	Native T1 mapping of autoimmune pancreatitis as a quantitative outcome surrogate. European Radiology, 2019, 29, 4436-4446.	4.5	8
46	Modified breathâ€hold compressedâ€sensing 3D MR cholangiopancreatography with a small fieldâ€ofâ€view and high resolution acquisition: Clinical feasibility in biliary and pancreatic disorders. Journal of Magnetic Resonance Imaging, 2018, 48, 1389-1399.	3.4	27
47	Liposomal nanohybrid cerasomes targeted to PD-L1 enable dual-modality imaging and improve antitumor treatments. Cancer Letters, 2018, 414, 230-238.	7.2	63
48	PD-1 blockade in combination with zoledronic acid to enhance the antitumor efficacy in the breast cancer mouse model. BMC Cancer, 2018, 18, 669.	2.6	20
49	A novel approach to monitoring the efficacy of anti-tumor treatments in animal models: combining functional MRI and texture analysis. BMC Cancer, 2018, 18, 833.	2.6	3
50	Combined use of iterative reconstruction and monochromatic imaging in spinal fusion CT images. Acta Radiologica, 2017, 58, 62-69.	1.1	12
51	Prospective comparison of biphasic contrastâ€enhanced CT, volume perfusion CT, and 3 Tesla MRI with diffusionâ€weighted imaging for insulinoma detection. Journal of Magnetic Resonance Imaging, 2017, 46, 1648-1655.	3.4	32
52	Microsurgery guided by sequential preoperative lymphography using 68Ga-NEB PET and MRI in patients with lower-limb lymphedema. European Journal of Nuclear Medicine and Molecular Imaging, 2017, 44, 1501-1510.	6.4	23
53	Insulinoma Detection With MDCT: Is There a Role for Whole-Pancreas Perfusion?. American Journal of Roentgenology, 2017, 208, 306-314.	2.2	19
54	Nuclear and Fluorescent Labeled PD-1-Liposome-DOX- ⁶⁴ Cu/IRDye800CW Allows Improved Breast Tumor Targeted Imaging and Therapy. Molecular Pharmaceutics, 2017, 14, 3978-3986.	4.6	66

#	Article	IF	CITATIONS
55	Head and neck angiography at 70ÂkVp with a third-generation dual-source CT system in patients: comparison with 100ÂkVp. Neuroradiology, 2017, 59, 1071-1081.	2.2	12
56	Improved resection and prolonged overall survival with PD-1-IRDye800CW fluorescence probe-guided surgery and PD-1 adjuvant immunotherapy in 4T1 mouse model. International Journal of Nanomedicine, 2017, Volume 12, 8337-8351.	6.7	19
57	Correlation Between Dual-energy and Perfusion CT in Patients with Focal Liver Lesions Using Third-generation Dual-source CT Scanner. Zhongguo Yi Xue Ke Xue Yuan Xue Bao Acta Academiae Medicinae Sinicae, 2017, 39, 74-79.	0.2	1
58	Bone Marrow Imaging by Third-generation Dual-source Dual-energy CT Using Virtual Noncalcium Technique for Assessment of Diffuse Infiltrative Lesions of Multiple Myeloma. Zhongguo Yi Xue Ke Xue Yuan Xue Bao Acta Academiae Medicinae Sinicae, 2017, 39, 114-119.	0.2	3
59	Third-generation Dual-source CT for Head and Neck CT Angiography with 70 kV Tube Voltage and 20-25 ml Contrast Medium in Patients With Body Weight Lower than 75 kg. Zhongguo Yi Xue Ke Xue Yuan Xue Bao Acta Academiae Medicinae Sinicae, 2017, 39, 4-8.	0.2	1
60	Feasibility of Pediatric Chest CT Using Spectral Filtration on Third-generation Dual-source CT. Zhongguo Yi Xue Ke Xue Yuan Xue Bao Acta Academiae Medicinae Sinicae, 2017, 39, 21-27.	0.2	1
61	Initial Experience of the Application of Automated Tube Potential Selection Technique in High-pitch Dual-source CT Angiography of Whole Aorta Using Third-generation Dual-source CT Scanner. Zhongguo Yi Xue Ke Xue Yuan Xue Bao Acta Academiae Medicinae Sinicae, 2017, 39, 62-67.	0.2	0
62	Initial Experience of the Application of Third-generation Dual-source CT Scanner in High-pitch Angiography of Aorta. Zhongguo Yi Xue Ke Xue Yuan Xue Bao Acta Academiae Medicinae Sinicae, 2017, 39, 68-73.	0.2	1
63	Characteristics of CT Perfusion Parameters of Focal Pancreatic Lesions and Data Comparison of Different Algorithms. Zhongguo Yi Xue Ke Xue Yuan Xue Bao Acta Academiae Medicinae Sinicae, 2017, 39, 80-87.	0.2	0
64	Comparison of Topogram-based Automated Selection of Tube Potential and Fixed Tube Potential in Imaging Solid Pancreatic Lesions. Zhongguo Yi Xue Ke Xue Yuan Xue Bao Acta Academiae Medicinae Sinicae, 2017, 39, 88-94.	0.2	0
65	Application of Low Tube Voltage 70 kV and Advanced Modeled Iterative Reconstruction in the Third-generation Dual-source CT to CT Colonography. Zhongguo Yi Xue Ke Xue Yuan Xue Bao Acta Academiae Medicinae Sinicae, 2017, 39, 95-100.	0.2	1
66	Feasibility Study of Low-dose Prostate CT Perfusion on Third-generation Dual-source CT. Zhongguo Yi Xue Ke Xue Yuan Xue Bao Acta Academiae Medicinae Sinicae, 2017, 39, 101-106.	0.2	0
67	Feasibility of Peripheral Artery CT Angiography under 70 kV with 50 ml Contrast Medium on the Third-generation Dual-source CT. Zhongguo Yi Xue Ke Xue Yuan Xue Bao Acta Academiae Medicinae Sinicae, 2017, 39, 107-113.	0.2	1
68	Coexpression of EGFR and CXCR4 Predicts Poor Prognosis in Resected Pancreatic Ductal Adenocarcinoma. PLoS ONE, 2015, 10, e0116803.	2.5	15
69	Spectrum of IgG4-related disease on multi-detector CT: a 5-year study of a single medical center data. Abdominal Imaging, 2015, 40, 3104-3116.	2.0	6
70	The image variations in mastoid segment of facial nerve and sinus tympani in congenital aural atresia by HRCT and 3D VR CT. International Journal of Pediatric Otorhinolaryngology, 2015, 79, 1412-1417.	1.0	4
71	Feasibility of Low-Dose Contrast Medium High Pitch CT Angiography for the Combined Evaluation of Coronary, Head and Neck Arteries. PLoS ONE, 2014, 9, e90268.	2.5	14
72	Incorporating MRI structural information into bioluminescence tomography: system, heterogeneous reconstruction and in vivo quantification. Biomedical Optics Express, 2014, 5, 1861.	2.9	22

#	Article	IF	CITATIONS
73	Histogram analysis of apparent diffusion coefficient for the assessment of local aggressiveness of cervical cancer. Archives of Gynecology and Obstetrics, 2014, 290, 341-348.	1.7	62
74	Primary pulmonary artery chondrosarcoma: the use of different imaging modalities. Chinese Medical Journal, 2014, 127, 2868-9.	2.3	0
75	Diagnosis and treatment of hepatic angiomyolipoma. Hepatobiliary Surgery and Nutrition, 2012, 1, 19-24.	1.5	10